SCIENTIFIC REPORTS

OPEN

SUBJECT AREAS:
ELECTRONIC PROPERTIES AND MATERIALS
SURFACES, INTERFACES AND THIN FILMS

Received
6 February 2014

Accepted
6 October 2014

Published
27 October 2014

Correspondence and requests for materials should be addressed to N.B. (nicolas.bergeal@espci.fr)

# Limit of the electrostatic doping in two-dimensional electron gases of $LaXO_3$(X = Al, Ti)/$SrTiO_3$

J. Biscaras[1], S. Hurand[1], C. Feuillet-Palma[1], A. Rastogi[2], R. C. Budhani[2,3], N. Reyren[4], E. Lesne[4], J. Lesueur[1] & N. Bergeal[1]

[1]LPEM-UMR8213/CNRS-ESPCI ParisTech-UPMC, 10 rue Vauquelin-75005 Paris, France, [2]Condensed Matter-Low Dimensional Systems Laboratory, Department of Physics, Indian Institute of Technology Kanpur, Kanpur 208016, India, [3]National Physical Laboratory, New Delhi - 110012, India and, [4]Unité Mixte de Physique CNRS-Thales, 1 Av. A. Fresnel, 91767 Palaiseau, France.

**In $LaTiO_3/SrTiO_3$ and $LaAlO_3/SrTiO_3$ heterostructures, the bending of the $SrTiO_3$ conduction band at the interface forms a quantum well that contains a superconducting two-dimensional electron gas (2-DEG). Its carrier density and electronic properties, such as superconductivity and Rashba spin-orbit coupling can be controlled by electrostatic gating. In this article we show that the Fermi energy lies intrinsically near the top of the quantum well. Beyond a filling threshold, electrons added by electrostatic gating escape from the well, hence limiting the possibility to reach a highly-doped regime. This leads to an irreversible doping regime where all the electronic properties of the 2-DEG, such as its resistivity and its superconducting transition temperature, saturate. The escape mechanism can be described by the simple analytical model we propose.**

Two-dimensional electron gases (2-DEGs) at $LaAlO_3/SrTiO_3$ and $LaTiO_3/SrTiO_3$ oxide interfaces[1] have attracted much attention since their electronic properties display a very rich physics with various electronic orders such as superconductivity[2–4] and magnetism[5–8]. In these structures, the 2-DEG is confined in an interfacial quantum well that typically extends on the order of 10 nm into the $SrTiO_3$ substrate at low temperature[2,4,9–11]. Applying a back-gate voltage enables to control electrostatically the filling of the well and thus modulate the 2-DEG electronic properties[12–14]. This exciting feature opens new avenues for studying the electronic orders and quantum phase transitions[15] in theses structures, as well as for developing oxide-based electronics that could make use of them[16–19]. Of particular interest, it was shown that adding electron to the well, increases continuously the electronic mobility and the strength of the Rashba spin-orbit coupling[14,20,21]. Also of interest, is the fact that the superconducting transition temperature of the 2-DEG exhibits a dome-like shape with a maximum $T_c$ of 200–300 mK at optimal doping[13,14]. Because of these remarkable properties, the highly-doped regime must be explored in further detail. However, the overdoped side of the dome seems particularly difficult to study because of unexplained saturation and hysteresis of the physical properties[13,14,20]. As of yet, this region is not fully understood. These observations raise a fundamental question: how much one can electrostatically dope the 2-DEG at oxides interfaces?

Although several theoretical descriptions of $LaXO_3$(X = Al, Ti)/$SrTiO_3$ interfaces have been proposed[22–27], the exact interfacial band structure remains controversial. Regardless of the calculation method and for the sake of clarity, in the present report we will consider a simple generalized situation where the bending of the $SrTiO_3$ conduction band defines a quantum well that accommodates discrete electronic sub-bands. To illustrate this point, we show in the Figure 1 the type of result that can be obtained by using a semiconductor approach in which we solve self-consistent Schrödinger-Poisson equations[14,28]. In this example, six sub-bands are filled and the higher energy one extends within 5 nm in the $SrTiO_3$[10,11]; this situation corresponds to a carrier density of approximately $7 \times 10^{13}$ $e^-/cm^2$, typical of values found in the literature. The effect of a back gate voltage on the interface is twofold: (i) it adds electrons to the well as the gate voltage increases ($\Delta V_G > 0$) and removes electrons from the well as the gate voltage decreases ($\Delta V_G < 0$), (ii) it controls the shape of the upper part of the well by tilting the conduction band profile in the substrate. Figure 2 shows illustrations of quantum well energy profiles that describe these different situations. As long as the Fermi level remains deep in the well, electrostatic gating can reversibly empty and fill the well as in the well-known semiconductors quantum wells. However, when the Fermi level rises to the top of the well, we no longer expect the doping to be possible. In this article we show

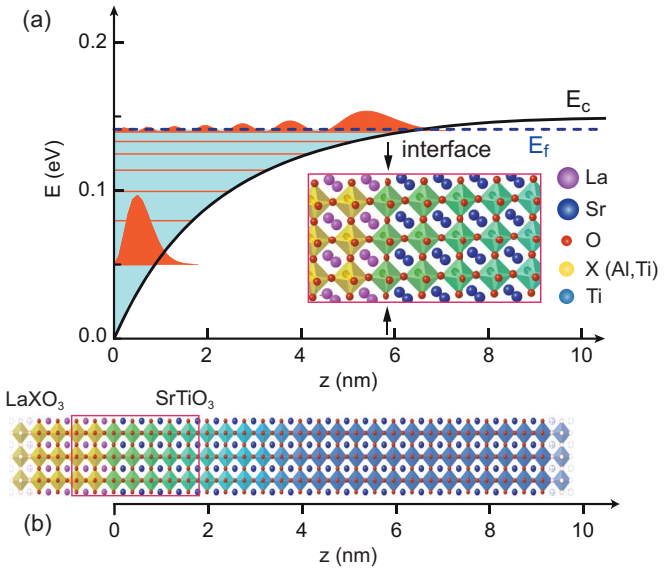


**Figure 1** | (a) Theoretical calculation of the quantum well profile at an $LaXO_3$(X = Al, Ti)/$SrTiO_3$ interface for a sample with a carrier density of $7.3 \times 10^{13}$ $e^-/cm^2$. Shown are the $SrTiO_3$ conduction band profile $E_C$ (black), the Fermi energy $E_F$ (blue dashed line) and the subbands energies (red) as a function of depth $z$ from the interface. Only light $d_{xy}$ electron bands have been taken into account to illustrate the quantum well (see Model and Discussion part for more details). The square modulus of the envelope function of the first and last filled sub-bands are indicated in arbitrary units (red areas). (b) and inset of panel (a): Schematic description of the crystallographic structure at interface.

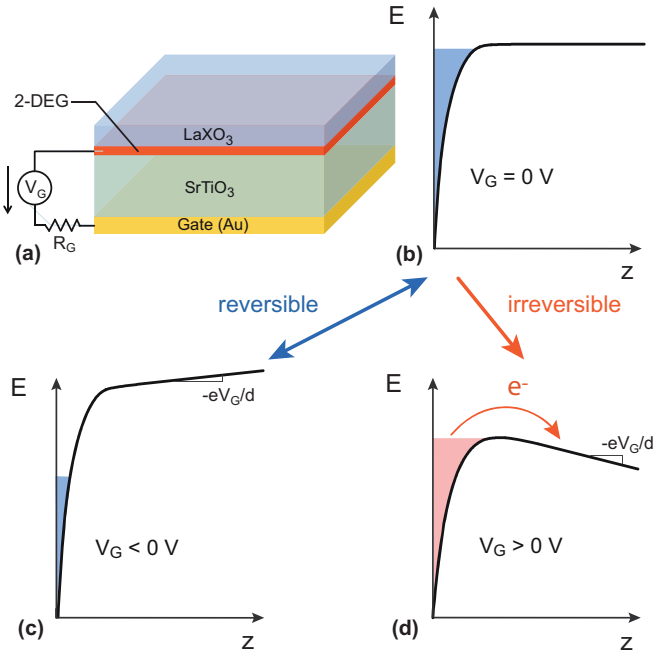


**Figure 2** | (a) Schematic of an $LaXO_3$(X = Al, Ti)/$SrTiO_3$ sample with a metallic back gate. (b,c,d) Illustration of filling the quantum well for different $V_G$ regimes. Starting from $V_G = 0$, applying a negative gate voltages $V_G < 0$ reversibly empties and fills the well. In contrast, applying the first positive polarisation ($V_G > 0$), causes electrons to irreversibly escape from the well. The slope $-eV_G/d$ (where $d = 500$ $\mu$m is the thickness of the $SrTiO_3$ substrate) of the conduction band is indicated.

that in $LaXO_3$(X = Al, Ti)/$SrTiO_3$ heterostructures, the Fermi energy lies intrinsically near the top of the well and that, beyond a filling threshold, additional electrons irreversibly escape from the well, hence limiting the possibility to reach a highly-doped regime. This behaviour can be described by a simple analytical model based on a thermal activated mechanism.

## Results

**First positive polarization.** In these experiments we used $LaTiO_3$ and $LaAlO_3$ epitaxial layers grown on $TiO_2$-terminated $SrTiO_3$ single crystals by Pulsed Laser Deposition as described in the Methods section. The samples had typical dimensions of $1 \times 2$ $mm^2$ and each had a metallic back-gate deposited at the rear of the 0.5 mm thick $SrTiO_3$ substrate. Before cooling, samples are kept in the dark for more than twelve hours to suppress any photoconductive effects. We studied the transport properties of $LaXO_3$(X = Al, Ti)/$SrTiO_3$ heterostructures at 4.2 K while applying a positive gate voltage for the first time, referred to as the first positive polarization. We first focus on the response of the $LaTiO_3$/$SrTiO_3$ sample shown in Figure 3. In this sample, increasing the gate voltage causes the resistance of the 2-DEG, after decreasing slightly, to saturate quickly and become independent of gate voltage. This behaviour is unexpected because, according to electrostatic laws, more electrons are added to the 2-DEG and therefore the resistance should decrease. This first positive polarization is irreversible: when the gate voltage is decreased from its maximum at $V_G^{max} = +200$ V, the reverse resistance curve deviates from the first forward curve. The carrier density $n$ was extracted from a two-carrier analysis of the Hall effect at high magnetic field (45 T) as described in reference [14] and Supplementary material. It was found to be constant during the first positive polarization, a behaviour consistent with the saturation of the resistance. Similar to the resistance curve, when the gate voltage is decreased after being increased to $V_G^{max} = +200$ V, the reverse carrier density curve does not follow the first forward curve. These two behaviours are in agreement with the irreversible situation described in Figure 2d. After the heterostructure is initially cooled, its Fermi level lies very close to the top of the well. Increasing the gate voltage adds electrons at the interface that quickly fills the highest energy sub-bands at the top of the well. After a certain time, these electrons eventually escape into the conduction band of the $SrTiO_3$ substrate, causing the saturation of the carrier density and the resistance of the 2-DEG. Note that this saturation is not associated with an increase of the gate current, suggesting that charges are trapped in the system.

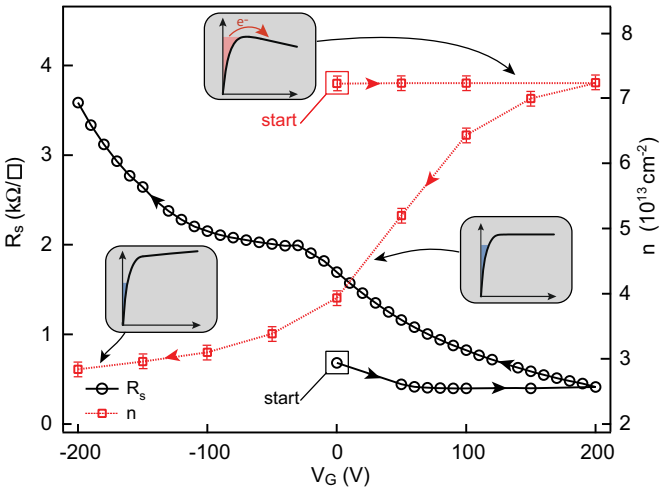


**Figure 3** | **Resistance of the 2-DEG (left axis) and carrier density $n$ (right axis) as functions of gate voltage measured for the first forward sweep (first positive polarization) and reverse sweep.** The starting points and the directions of the sweeps are indicated by enclosing boxes and arrows respectively.

Beyond our initial experiments, we studied the irreversibility of the first positive polarization in further detail. After cooling a $LaTiO_3$/$SrTiO_3$ heterostructure to 4.2 K, we measured its sheet resistance as a function of gate voltage by using different polarization procedures (Fig. 4a). Different from our previous measurements, in this experiment we applied a negative first polarization down to $V_G^{min} = -200$ V. Doing so increased the resistivity – an expected behaviour, as electrons are removed from the 2-DEG – and we observed no saturation. As the voltage returns to $V_G = 0$ V, the forward resistance curve appears to match the first reverse curve. However, when the gate voltage is further increased to the value $V_G^{max1} = +50$ V and then decreased back to $V_G = -200$ V, the reverse resistance curve deviates from the first forward curve. This new curve is fully reversible as long as the gate voltage is not increased above $V_G^{max1}$. We replicated this pattern with increasing maximum gate voltages of $V_G$ ($V_G^{max2} = +100$ V, and $V_G^{max3} = +200$ V).

These results show that the well can be emptied ($\Delta V_G < 0$) and filled ($\Delta V_G > 0$) reversibly as long as the gate voltage is not increased beyond a critical value corresponding to the maximum value $V_G^{max}$ previously applied to the metallic gate, a situation in which the Fermi level reaches the top of the well. Beyond this maximum value, we expect electrons to escape irreversibly from the 2-DEG into the $SrTiO_3$ substrate. We performed the same measurements on an $LaAlO_3$/$SrTiO_3$ sample and we observed similar results (Fig. 5a). For this sample, the irreversible regime is reached at a gate voltage of 50 V indicating that the Fermi level after the initial cooling was slightly below the top of the well. As a consequence, at lower temperatures, the superconducting transition temperature saturates beyond this gate value (Fig. 5b and inset). To suppress the undesirable hysteresis effects, a first positive polarisation can be used as a forming process of the quantum well prior to other measurements[13,14,20]. However, in any case, the heavy doping of the 2-DEG will always be limited because the Fermi level cannot exceed the top of the quantum well.

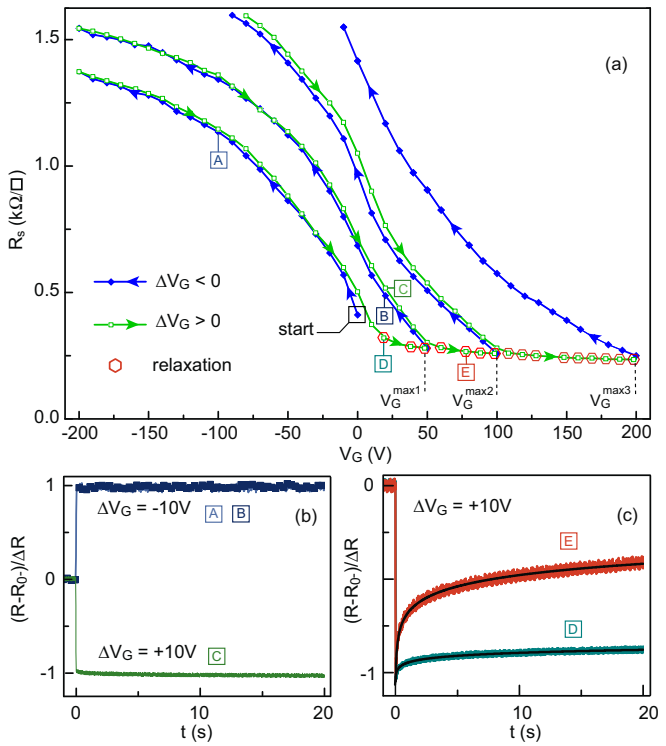


**Figure 4 | Resistance of the $LaTiO_3$/$SrTiO_3$ sample measured for several forward sweeps ($\Delta V_G > 0$) and reverse sweeps ($\Delta V_G < 0$) with a starting $V_G$ of 0 V ("start" point).** We first sweep the $V_G$ to −200 V and then increase it to a maximum value $V_G^{max1}$ before sweeping it back to −200 V. We repeated this operation with increasing gate voltage maximum of $V_G^{max2}$ and $V_G^{max3}$. Red markers indicate the region in which we observed relaxation. (b) Normalized resistance over time measured as a function of time after a $\Delta V_G = \pm 10$ V step in points labelled "A", "B" and "C" on the $R(V_G)$ curves of panel (a). (c) Normalised resistance over time after a $\Delta V_G = +10$ V step at points labelled "D" and "E" on the $R(V_G)$ curves in (a). The resistance relaxation is fitted to a logarithm with form $\alpha + \beta \log(t)$ (solid black lines).

**Time-dependent measurement.** We performed time-dependent resistivity measurements to assess how the 2-DEG responds to gate voltage steps of $\Delta V_G = \pm 10$ V. The expected corresponding modification of the carrier density is $\Delta n = C_a \Delta V_G / e$ where $C_a$ is the capacitance per unit of area of the $SrTiO_3$ substrate. Representative results of these measurements are shown in Figure 4b and 4c for different filling situations, labelled "A", "B", "C", "D" and "E" in Figure 4a. In the reversible regime, the resistance shows clears $\Delta R$ jumps before reaching a stable value (Fig. 4b). As expected, $\Delta R$ is positive when electrons are removed ($\Delta V_G = -10$ V, labels "A" and "B") and negative when electrons are added ($\Delta V_G = +10$ V, label "C"). In contrast, after applying a voltage step of $\Delta V_G = +10$ V in the irreversible regime, the initial negative jump is followed

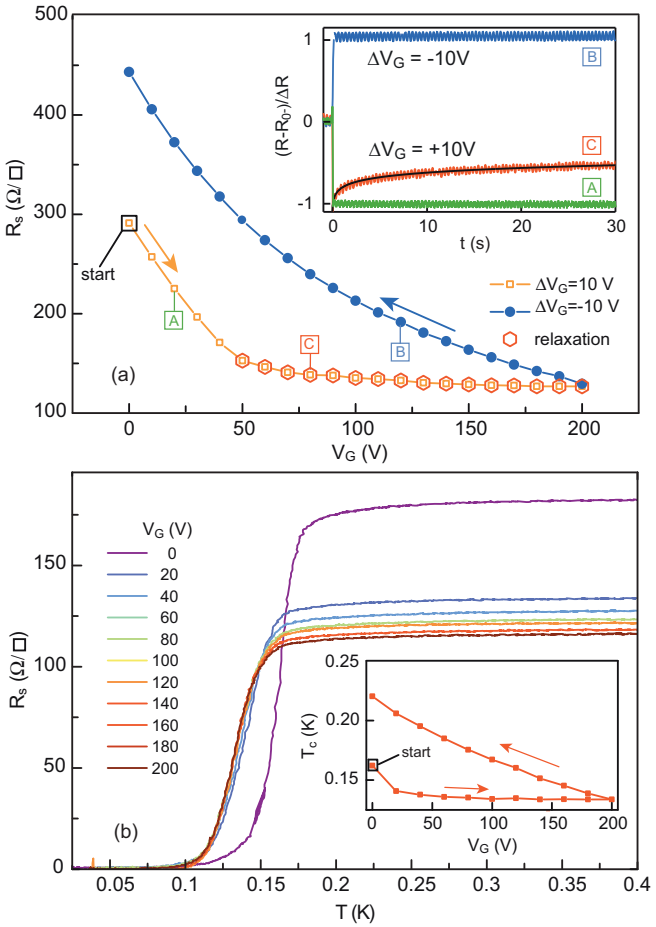


**Figure 5 |** (a) Sheet resistance of the $LaAlO_3$/$SrTiO_3$ sample during the first positive polarization at 4.2 K. Inset: Normalised resistance over time after a $\Delta V_G = \pm 10$ V step for points labelled "A", "B" and "C" on the $R(V_G)$ curves in the main panel. The relaxation of the resistance is fitted to a logarithm with the form $\alpha + \beta \log(t)$. (b) Sheet resistance of the $LaAlO_3$/$SrTiO_3$ sample as a function of temperature for different $V_G$ values during the first positive polarization, showing the saturation of $T_c$. Inset: Hysteresis of $T_c$ as a function of $V_G$ for the first positive polarization.

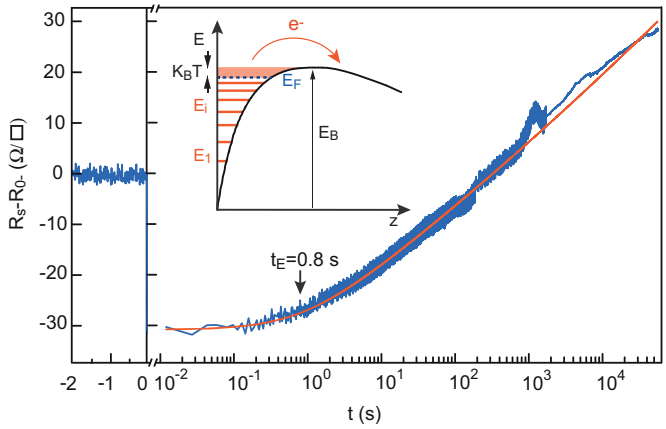


**Figure 6 | Resistance over time of the $LaTiO_3/SrTiO_3$ sample after a $\Delta V_G = +10$ V step at t = 0, fitted by equation (6).** The escape time $t_E$ is 0.8 ± 0.1 s. Inset: Schematic of the situation considered to model the thermal escape of the electrons from the well.

by a slow increase of the resistance (Fig. 4c, labels "D" and "E"). We interpret this behaviour as the sign that electrons added to the 2-DEG by the gate-voltage step, eventually escaped from the well. By a first approximation, the resistance relaxation follows a logarithmic time dependence with the form $\alpha + \beta \log(t)$. This relaxation must not be confused with the charging time of the capacitor $R_G C_a A$ (A is the area of the sample) which is always present at a much shorter time scale (see Supplementary Information).

## Model and Discussion

To analyze the relaxation in the irreversible regime we propose a model that describes the dynamics of electrons escaping from the well. We consider a 2D quantum well at the interface with an infinite barrier on the $LaXO_3$(X = Al, Ti) side and a barrier of finite height $E_B$ on the $SrTiO_3$ side (Inset of Fig. 6). A number $n_L$ of 2D parabolic subbands with energy $E_i$ ($i = 1,\ldots,n_L$) and density of states $N = m/(\pi\hbar^2)$ are filled. We assume that at a temperature $T$, electrons at the Fermi level $E_F$ can jump over the barrier with first order kinetics:

$$\frac{dn}{dt} = -kn \tag{1}$$

where $n$ is the carrier density of the 2-DEG and $k$ is the kinetic factor. This latter follows an Arrhenius law: $k = ve^{-\frac{\Delta}{k_B T}}$ where the activation energy is $\Delta = E_B - E_F$, and $v$ is a characteristic frequency factor. In two dimensions, the electron density is given by

$$n = \sum_{i=1}^{n_L} N(E_F - E_i) = N_F(E_F - E_L) \tag{2}$$

where $N_F = n_L N$ is the total density of states at the Fermi energy and $E_L = \sum_{i=1}^{n_L} E_i/n_L$. This situation is formally equivalent to the one with a single band of energy $E_L$ and a density of state $N_F$. For a small variation of $n$, the temporal evolution of the Fermi energy is

$$\frac{dE_F}{dt} = -ve^{-\frac{E_B - E_F}{k_B T}}(E_F - E_L) \tag{3}$$

At low temperature ($k_B T \ll E_F - E_L$), a good approximate solution to equation (3) is

$$E_F(t) \approx E_F^{0^+} - k_B T \ln\left(1 + \frac{t}{t_E}\right) \tag{4}$$

where $E_F^{0^+}$ is the Fermi level at $t = 0^+$ (immediately after the voltage step, neglecting the short charging time $R_G C_a A$) and $t_E$ is the characteristic escape time given by

$$t_E = \frac{k_B T N_F}{v n_{0^+}} e^{\frac{E_B - E_F^{0^+}}{k_B T}} \tag{5}$$

where $n_{0^+}$ is the carrier density at $t = 0^+$. Therefore, the Fermi level is constant for $t < t_E$, after which it decreases logarithmically. From (2) and (4) we can obtain the temporal dynamics of the 2-DEG Drude resistivity as

$$R(t) = \frac{1}{e\mu n(t)} \approx R_{0_+}\left[1 + \frac{N_F k_B T}{n_{0^+}} \ln\left(1 + \frac{t}{t_E}\right)\right] \tag{6}$$

where $R_{0^+} = (e\mu n_{0^+})^{-1}$ is the resistivity at $t = 0^+$. In Figure 6 we show the resistance relaxation after a $\Delta V_G = +10$ V step; this relaxation agrees very well with equation (6) over more than six decades of time (10 ms to 14 hours). A direct consequence of the logarithmic relaxation is the absence of an asymptotic value. However, on a linear scale the resistance changes very slowly after a few minutes, which can give a false impression of saturation. We emphasise here that the peculiar form of relaxation given by Eq. 6 is specific to the case of a well that empties itself and cannot describe other thermally activated mechanisms.

To validate this model, we systematically studied how the relaxation depends on the polarization parameters. In particular, we measured the resistance relaxation after a $\Delta V_G = +10$ V step at different $V_G$ values (Fig. 7a), and for different steps of $\Delta V_G = 5$, 10, 20 and 40 V (Fig. 7c). The experimental data from both experiments agree with the theoretical equation (6), confirming that the model describes the phenomena we observed very well. We also observed the same agreement between experimental data and theoretical expectations for the $LaAlO_3/SrTiO_3$ sample (Supplementary Material). To understand how the escape time depends on $V_G$ and $\Delta V_G$, we can express equation (5) as

$$\ln t_E = \gamma - \kappa C_a(V_G)\Delta V_G \tag{7}$$

where $\gamma$ and $\kappa$ are constants whose expressions can be found in the Supplementary Material. Because the dielectric constant of $SrTiO_3$ is electric-field-dependent, the capacitance $C_a$ changes with gate voltage[29]. Therefore, the number of charges added by a constant voltage step $\Delta V_G$ depends on the absolute value of the gate voltage. Figure 7b shows the linear variation of $\ln t_E$ as a function of $C_a$ as expected from equation (7). We also found $\ln t_E$ to vary linearly with $\Delta V_G$ for small gate voltage step $\Delta V_G$ (figure 7d). For larger steps, the electrons are injected very high in the well complicating our determination of the short $t_E$ values.

In the limit $t \gg t_E$, equation (6) reduces to $R(t) = \alpha + \beta \log t$ where $\beta = \frac{N_F k_B T R_{0^+}}{2.3 n_{0^+}}$. Figure 8a and 8b show that the $\beta$ parameter increases linearly with temperature, as expected for a thermally activated mechanism. As already mentioned, electrons escaping into the $SrTiO_3$ substrate get trapped by the defects of the crystal and no longer contribute to electronic transport. They can be released into the 2-DEG if the temperature of the sample increases above two characteristic values $T_1 \approx 70$ K and $T_2 \approx 170$ K for our $LaTiO_3/SrTiO_3$ sample (Fig. 8b). The trapping energy inferred from the temperature $T_1$ is approximately 6 meV. As the electrons are trapped at a typical distance $t$ from the interface comparable to the quantum well extension (~10 nm) which is much smaller than the thickness $d = 500$ μm of the $SrTiO_3$ substrate, it is not possible to de-trapp the electrons with a negative gate voltage of reasonable value. Indeed, the potential energy transferred the electrons $eV_G \times t/d$ always remains negligible compare to the trapping one. For this reason we do not observe hysteresis for negative gate voltages.

The same de-trapping behaviour has also been reported in $LaAlO_3/SrTiO_3$[30] at similar temperatures. The authors associated this behaviour to a thermally activated mechanism supported by exponential relaxations of conductivity near 70 K and 160 K. However,

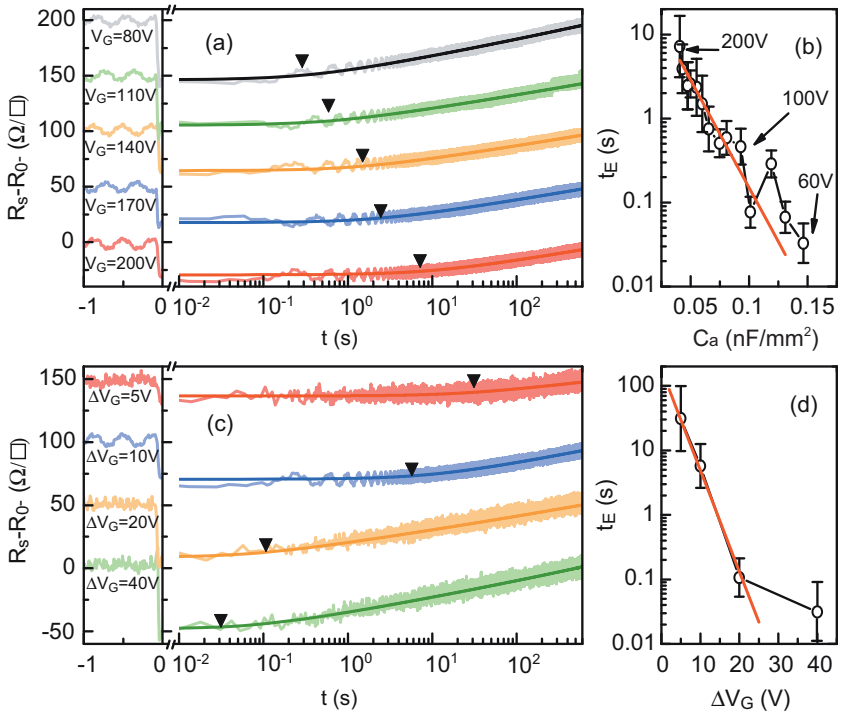


**Figure 7** | (a) Resistance over time of the $LaTiO_3/SrTiO_3$ sample, measured at 4.2 K for different gate voltages after a $\Delta V_G = +10$ V step, fitted by equation (6). Arrows indicate $t_E$ values extracted from the fits. (b) Logarithm of $t_E$, plotted as a function of $C_a$ and fitted with equation (7) (red line). (c) Resistance over time, measured at 4.2 K for different steps $\Delta V_G$, and fitted with equation (6). Arrows indicate $t_E$ values extracted from the fits. (d) Logarithm of $t_E$ plotted as a function of $\Delta V_G$ and fitted with equation (7).

this behaviour should not be confused with the low-temperature logarithmic relaxations observed after a gate voltage step that we described in the present article. The relaxations at 70 K and 160 K are caused by thermal escape of electrons from traps with well-defined energy barriers, giving single exponential relaxations. In contrast, the low-temperature relaxations during the first positive polarisation are caused by electrons escaping from the quantum well with a time-dependent energy barrier, leading to logarithmic time dependence after a characteristic escape time. Similarly, relaxations associated to photoconductivity[32,33] or relaxations sometimes observed at high temperature in $SrTiO_3$ based structures and attributed to anions or vacancy diffusion[12,31] also differ from the behaviour discussed in the present article.

In this article, we have taken into account only light electron bands to illustrate the quantum well. Note that the escape mechanism described here is inherent to the presence of a quantum well at the $LaXO_3$(X = Al, Ti) $SrTiO_3$ interface, disregarding the details of the band structure. It will remain valid even in the presence of a heavy band that has been theoretically predicted[22,25,27] and seen by ARPES measurements to a certain extent[38], since all the sub-bands cross the Fermi level (see Supplementary Figure S4). The escape mechanism does not depend on the exact shape of the potential well, which can be slightly modified by the presence of non-mobile charges at the interfaces (trapped electrons, impurities…) and can vary from sample to sample. It also does not depend strongly on the absolute carrier density of the as-grown sample since the location of the Fermi energy close to the top of quantum well at zero gate voltage is a simple consequence of the Poisson's equation.

In summary, we have shown that in $LaAlO_3/SrTiO_3$ and $LaTiO_3/SrTiO_3$ heterostructures, the Fermi level is instrinsically close to the top of the quantum well after the cool-down. When the carrier density is increased by an electrostatic back-gate voltage beyond a critical value, electrons escape into the $SrTiO_3$ substrate at a rate well explained by a thermally activated leakage from the well. This phenomenon which appears both in $LaAlO_3/SrTiO_3$ and $LaTiO_3/SrTiO_3$ heterostructures, is directly responsible for the saturation of the 2-DEG properties with gate voltage, including the mobility and the carrier density, as well as the superconducting transition temperature observed at lower temperature. The exact capacity of the well– and, thus, the maximum carrier density– is mainly determined by growth conditions and can vary from sample to sample. While it is possible to deplete reversibly the quantum well by electrostatic back-gating, the filling is limited by the intrinsic location of the Fermi energy. To overcome this problem we suggest using double gated structures: A back gate could be used to engineer the shape of the quantum well which determines the carrier mobility through the bending of the $SrTiO_3$ conduction band. In conjunction, a top gate can be used to add electrons to the well[34,35].

## Methods

**Growth of the heterostructures.** $LaTiO_3/SrTiO_3$ hetero-structures were grown at ITT Kanpur (India) using excimer laser based PLD system on commercially available (Crystal GmbH Germany) single crystal substrates of $SrTiO_3$ (100) oriented. The substrates were treated with buffered HF to expose $TiO_2$ terminated surface. Before deposition, the substrates were heated to 850–950°C for one hour in an oxygen pressure of 200 mTorr to realize surface reconstruction. The source of $LaTiO_3$ was a stoichiometric sintered target of 22 mm in diameter which was ablated in an oxygen partial pressure of $1 \times 10^{-4}$ Torr with energy fluence of 1 J/cm$^2$ per pulse at a repetition rate of 3 Hz to achieve a growth rate of 0.12 Å/s. Under these conditions, the $LaTiO_3$ phase is grown on $SrTiO_3$ substrates, as shown by X-Rays diffraction patterns[4]. In this study, we used 15 u.c. thick $LaTiO_3$ layers on 0.5 mm thick $SrTiO_3$ substrates.

$LaAlO_3/SrTiO_3$ heterostructures were fabricated at UMR CNRS/Thales (Paris, France). A thin $LaAlO_3$ film was deposited by PLD (Surface PLD system) on a $TiO_2$-terminated (001)-oriented $SrTiO_3$ substrate (Crystec and SurfaceNet). A buffered HF treatment followed by annealing, as described in Ref. [36], was used to obtain the $TiO_2$ termination required to obtain the conducting electronic system at the interface. The KrF excimer (248 nm) laser ablates the single-crystalline $LaAlO_3$ target at 1 Hz, with a fluence between 0.6 and 1.2 J/cm$^2$ in an $O_2$ pressure of $2 \times 10^{-4}$ mbar. The substrate was typically kept at 730C° during the growth, monitored in real-time by RHEED. As the growth occurs layer-by-layer, it allows us to control the thickness at the unit cell level. After the growth of the film, the sample is cooled down to 500°C in $10^{-1}$ mbar of $O_2$, where the oxygen pressure is increased up to 400 mbar. To reduce the presence of oxygen vacancies (in both the substrate and the film), the sample stays in these

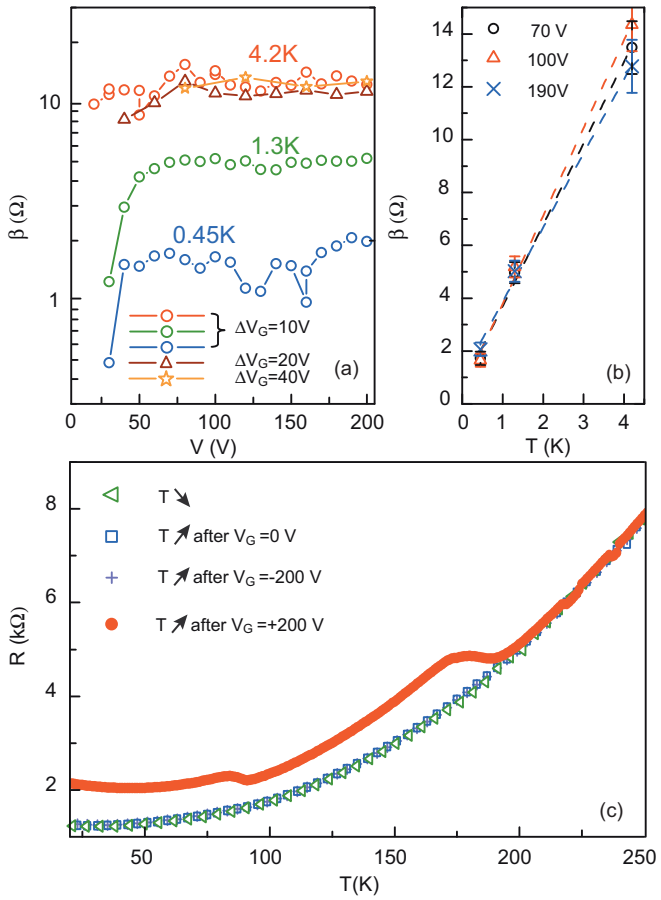


**Figure 8** | (a) Parameter $\beta$ of the logarithmic fit of the relaxation curves, as a function of gate voltage for three different temperatures and different values of $\Delta V_G$. (b) Parameter $\beta$ (symbols) as a function of temperature for three selected gate voltages. The dashed lines correspond to a linear fit. (c) Resistance as a function of temperature measured for different sweep procedures: cooling down (triangle) and warming up (square) at $V_G = 0$ (square), warming up with $V_G = 0$ after a sweep to $V_G = -200$ V (cross) and warming up with $V_G = 0$ after a sweep to $V_G = +200$ V (circle).

conditions for 30 minutes before being cooled down to room temperature[37]. The substrate-target distance was about 57 mm, leading to a growth rate of about 0.2 Å/s in the above conditions. In this study, we used 5 u.c. thick $LaAlO_3$ layers on 0.5 mm thick $SrTiO_3$ substrates.


1. Ohtomo, A. & Hwang, H. Y. A high-mobility electron gas at the *LaAlO$_3$/SrTiO$_3$* heterointerface. *Nature* **427**, 423–426 (2004).
2. Reyren, N. *et al.* Superconducting interfaces between insulating oxides. *Science* **317**, 1196–1199 (2007).
3. Perna, P. *et al.* Conducting interfaces between band insulating oxides: The *LaGaO$_3$/SrTiO$_3$* heterostructure. *Appl. Phys. Lett.* **97**, 152111 (2010).
4. Biscaras, J. *et al.* Two-dimensional superconductivity at a Mott insulator/band insulator interface *LaTiO$_3$/SrTiO$_3$*. *Nature Commun.* **1**, 89 (2010).
5. Brinkman, A. *et al.* Magnetic effects at the interface between non-magnetic oxides. *Nature Mater.* **6**, 493–496 (2007).
6. Ben Shalom *et al.* Anisotropic magnetotransport at the *SrTiO$_3$/LaAlO$_3$* interface. *Phys. Rev. B* **80**, 140403 (2009).
7. Li, L., Richter, C., Mannhart, J. & Ashoori, R. C. Coexistence of magnetic order and two-dimensional superconductivity at *LaAlO$_3$/SrTiO$_3$* interfaces. *Nature Phys.* **7**, 762–766 (2011).
8. Bert, J. A. *et al.* Direct imaging of the coexistence of ferromagnetism and superconductivity at the *LaAlO$_3$/SrTiO$_3$* interface. *Nature Phys.* **7**, 767–771 (2011).
9. Reyren, N. *et al.* Anisotropy of the superconducting transport properties of the *LaAlO$_3$/SrTiO$_3$* interface. *Appl. Phys. Lett.* **94**, 112506 (2009).
10. Copie, O. *et al.* Towards Two-Dimensional Metallic Behavior at *LaAlO$_3$/SrTiO$_3$* Interfaces. *Phys. Rev. Lett.* **102**, 216804 (2009).
11. Basletic, M. *et al.* Mapping the spatial distribution of charge carriers in *LaAlO$_3$/SrTiO$_3$* heterostructures. *Nature Mat.* **7**, 621–625 (2008).
12. Thiel, S., Hammerl, G., Schmehl, A., Schneider, C. W. & Mannhart, J. Electron Gases in Oxide Heterostructures. *Science* **313**, 1942–1945 (2006).
13. Caviglia, A. D. *et al.* Electric field control of the *LaAlO$_3$/SrTiO$_3$* interface ground state. *Nature* **456**, 624 (2008).
14. Biscaras, J. *et al.* Two-dimensional superconductivity induced by high-mobility carrier doping in *LaTiO$_3$/SrTiO$_3$* heterostructures. *Phys. Rev. Lett.* **108**, 247004 (2012).
15. Biscaras, J. *et al.* Multiple Quantum Criticality in a two-dimensional superconductor. *Nature Mat.* **12**, 542–548 (2013).
16. Bibes, M. Villegas, J. E. & Barthlmy, A. Ultrathin oxide films and interfaces for electronics and spintronics. *Adv. Phys.* **60**, 5–84 (2011).
17. Takagi, H. & Hwang, H. Y. An Emergent Change of Phase for Electronics. *Science* **327**, 1601–1602 (2010).
18. Mannhart, J. & Schlom, D. G. Oxide Interfaces - An Opportunity for Electronics. *Science* **327**, 1607–1611 (2010).
19. Hwang, H. Y. *et al.* Emergent phenomena at oxide interfaces. *Nature Mat.* **11**, 103–113 (2012).
20. Bell, C. *et al.* Dominant Mobility Modulation by the Electric Field Effect at the *LaAlO$_3$/SrTiO$_3$* Interface. *Phys. Rev. Lett.* **103**, 226802 (2009).
21. Caviglia, A. D. *et al.* Tunable Rashba Spin-Orbit Interaction at Oxide Interfaces. *Phys. Rev. Lett.* **104**, 126803 (2010).
22. Popovic, Z., Satpathy, S. & Martin, R. M. Origin of the Two-Dimensional Electron Gas Carrier Density at the $LaAlO_3$ on $SrTiO_3$ Interface. *Phys. Rev. Lett.* **101**, 256801 (2008).
23. Kancharla, S. S. & Dagotto, E. Metallic interface at the boundary between band and Mott insulators. *Phys. Rev. B* **74**, 195427 (2006).
24. Salluzzo, M. *et al.* Orbital Reconstruction and the Two-Dimensional Electron Gas at the *LaAlO$_3$/SrTiO$_3$* Interface. *Phys. Rev. Lett.* **102**, 166804 (2009).
25. Son, W.-J., Cho, E., Lee, B., Lee, J. & Han, S. Density and spatial distribution of charge carriers in the intrinsic n-type *LaAlO$_3$/SrTiO$_3$* interface. *Phys. Rev. B* **79**, 245411 (2009).
26. Delugas, P. *et al.* Spontaneous 2-Dimensional Carrier Confinement at the n-Type *SrTiO$_3$/LaAlO$_3$* Interface. *Phys. Rev. Lett.* **106**, 166807 (2011).
27. Park, S. Y. & Millis, A. J. Charge density distribution and optical response of the *LaAlO$_3$/SrTiO$_3$* interface. *Phys. Rev. B* **87**, 205145 (2013).
28. Meevasana, W. *et al.* Creation and control of a two-dimensional electron liquid at the bare *SrTiO$_3$* surface. *Nature Mater.* **10**, 114–118 (2011).
29. Neville, R. C., Hoeneisen, B. & Mead, C. A. Permittivity of Strontium Titanate. *J. Appl. Phys.* **43**, 2124 (1972).
30. Seri, S., Schultz, M. & Klein, L. Thermally activated recovery of electrical conductivity in *LaAlO$_3$/SrTiO$_3$*. *Phys. Rev. B* **87**, 125110 (2013).
31. Shultz, M. & Klein, L. Relaxation of transport properties in electron-doped *SrTiO$_3$*. *Appl. Phys. Lett.* **91**, 151104 (2007).
32. Rastogi, A., Pulikkotil, J. J., Auluck, S., Hossain, Z. & Budhani, R. C. Photoconducting state and its perturbation by electrostatic fields in oxide-based two-dimensional electron gas. *Phys. Rev. B* **86**, 075127 (2012).
33. Di Gennaro, E. *et al.* Persistent Photoconductivity in 2D Electron Gases at Different Oxide Interfaces. *Adv. Optical Mater.* **1**, 834–843 (2013).
34. Forg, B., Richter, C. & Mannhart, J. Field-effect devices utilizing *LaAlO$_3$ – SrTiO$_3$* interfaces. *Appl. Phys. Lett.* **100**, 053506 (2012).
35. Hosoda, M., Hikita, Y., Hwang, H. Y. & Bell, C. Transistor operation and mobility enhancement in top-gated *LaAlO$_3$/SrTiO$_3$* heterostructures. *Appl. Phys. Lett.* **103**, 103507 (2013).
36. Koster, G., Kropman, B. L., Rijnders, G. J. H. M., Blank, D H. A. & Rogalla, H. Quasi-ideal strontium titanate crystal surfaces through formation of strontium hydroxide. *Appl. Phys. Lett.* **73**, 2920 (1998).
37. Cancellieri, C. *et al.* Influence of the growth conditions on the *LaAlO$_3$/SrTiO$_3$* interface electronic properties. *Europhys. Lett.* **91**, 17004 (2010).
38. Berner, G. *et al.* Direct k-Space Mapping of the Electronic Structure in an Oxide-Oxide Interface. *Phys. Rev. Lett.* **110**, 247601 (2013).


## Acknowledgments

The authors gratefully thank M. Grilli and S. Caprara for stimulating discussions. High-magnetic field measurements were performed at the LNCMI Toulouse with the help of D. LeBoeuf and C. Proust. This work was supported by the french ANR and the Région Ile-de-France through CNano IdF and Sesame programs, as well as partially supported by Euromagnet II. The work at IIT Kanpur was funded by Council of Scientific and Industrial Research. R.C.Budhani acknowledges the J.C. Bose Fellowship from the Department of Science and Technology, Government of India.

## Author contributions

A.R. and R.C.B. prepared the $LaTiO_3/SrTiO_3$ samples. N.R. and E.L. prepared the $LaAlO_3/SrTiO_3$ samples. J.B. and S.H. performed the measurements, assisted by C.F.-P., J.B., J.L. and N.B. carried out the analysis of the results and wrote the article.

## Additional information

**Supplementary information** accompanies this paper at http://www.nature.com/scientificreports

**Competing financial interests:** The authors declare no competing financial interests.

**How to cite this article:** Biscaras, J. *et al*. Limit of the electrostatic doping in two-dimensional electron gases of $LaXO_3$(X = Al, Ti)/$SrTiO_3$. *Sci. Rep.* **4**, 6788; DOI:10.1038/srep06788 (2014).